

Uncovering Forbidden Optical Transitions in PbSe Nanocrystals

Jeffrey J. Peterson,[†] Libai Huang,[†] Christophe Delerue,[‡] Guy Allan,[‡] and Todd D. Krauss^{*,†}

Department of Chemistry, University of Rochester, Rochester, NY, and Institut d'Electronique, de Microélectronique et de Nanotechnologie (UMR CNRS 8520), Département ISEN, Lille Cedex, France

Received September 28, 2007; Revised Manuscript Received October 26, 2007

ABSTRACT

The $1S_{h,e}-1P_{e,h}$ exciton transition energy of PbSe nanocrystals was determined via two-photon photoluminescence excitation spectroscopy and was found to be in good agreement with predictions from a tight-binding calculation. The two-photon excitation peak occurs at energies very close to a strong feature in the one-photon absorption spectrum and suggests that it should be assigned as a formally forbidden S–P transition. Leading explanations for the unusual strength of the forbidden transition are discussed.

Interest in PbSe nanocrystals (NCs) has recently exploded, largely due to their enabling potential in various technological applications^{1–4} and for their utility in fundamental studies of quantum confinement effects.⁵ Because of the large electron and hole Bohr radii in the bulk crystal (23 and 23 nm, respectively), PbSe NCs can achieve significantly greater levels of quantum confinement than more commonly studied III–V and II–VI materials, and thus one expects PbSe NCs with a sparse electronic structure, consisting of widely separated electron and hole energy states. Indeed, colloidal PbSe NCs exhibit a series of well-defined and widely spaced peaks in their absorption spectra (Figure 1a).^{6–8} Despite this apparent simplicity, prominent spectral features are observed that appear to completely violate basic quantum mechanical principles, and in fact PbSe NCs have proven to be very complex materials for which a general understanding of even the most basic characterizations has remained controversial.

A variety of models have been used to describe PbSe NC's electronic structure.^{9–12} Employing a 4-band, $\mathbf{k}\cdot\mathbf{P}$ envelope-function formalism (i.e., the effective mass approximation, EMA), Kang and Wise accurately modeled the size-dependence of the energy of the first excitonic absorption feature over a wide range of PbSe NC sizes.⁹ Recent atomistic calculations of NC energy states using a tight-binding (TB) methodology by Allan and Delerue¹⁰ refined the energy gap's size dependence and included higher order effects resulting from PbSe's full band structure, rather than solely the band edge states that are modeled in the EMA calculation. Within both models, the energy level spacing

between the two lowest dipole-allowed transitions ($1S_h-1S_e$ and $1P_h-1P_e$) quantitatively agrees with the energies of the first and third peaks in the one-photon absorption spectrum (Figure 1b). However, both EMA and TB approaches fail to predict a dipole-allowed transition at the second absorption peak, which is experimentally observed to be quite strong. Surprisingly, the second transition energy is well predicted if selection rules are relaxed to allow the formally forbidden mixed parity transitions ($1P_h-1S_e$ and $1S_h-1P_e$), although a rationale for allowing such transitions has remained unclear.

Alternatively, recent scanning tunneling spectroscopy (STS) studies suggest that the second peak is the second dipole-allowed transition, $1P_h-1P_e$.¹³ Because STS is not sensitive to wavefunction symmetry, only local density of states, a precise STS analysis of energy level spacings is difficult. Still, this assignment provides a natural explanation for the observed transition strength and agrees well with recent pseudopotential calculations of PbSe NC electronic structure.¹¹ A principle difference between the pseudopotential and previous EMA/TB approaches is the prediction of a dense manifold of hole states due to coupling between multiple valence band maxima in the bulk band structure. Thus, despite over 15 years of study on lead–salt NCs, not only do the quantitative details of their absorption spectra remain elusive, but conflicting qualitative descriptions of their electronic structure persist as well.

An alternative technique that directly probes the $1S_{e,h}-1P_{h,e}$ transition and that has been successfully utilized to elucidate electronic structure details in CdSe and CuCl NCs is two-photon photoluminescence excitation spectroscopy (2PPLE).^{14–16} Compared to one-photon processes, two-photon processes obey an alternative set of quantum me-

* Corresponding author. E-mail: krauss@chem.rochester.edu.

[†] University of Rochester.

[‡] Institut d'Electronique, de Microélectronique et de Nanotechnologie.

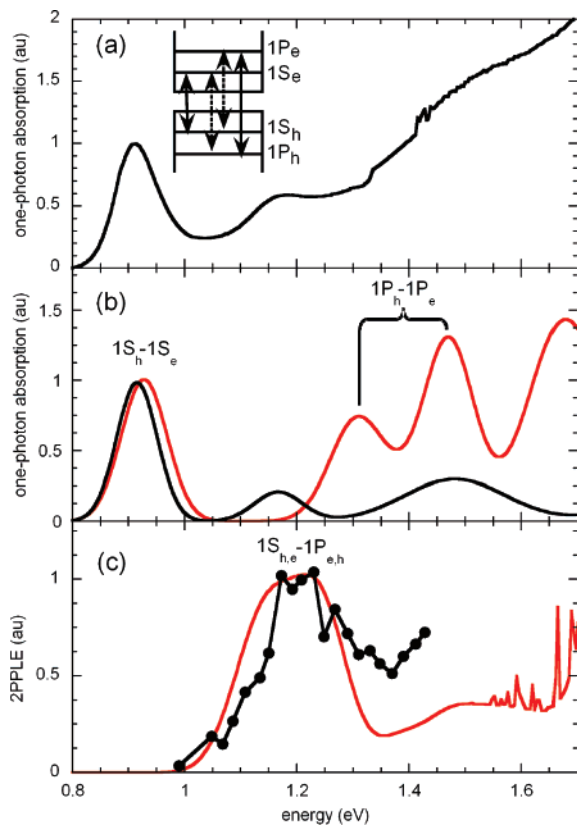


Figure 1. (a) One-photon absorption spectrum of PbSe NCs with the first exciton peak at 0.911 eV. (Inset) Energy level diagram of PbSe NCs, indicating one-photon-allowed (solid arrows) and two-photon-allowed (dashed arrows) transitions. (b) Experimental one-photon absorption peaks obtained after subtracting an increasing polynomial background (black line) and calculated one-photon peaks (red line) from a TB model. (c) Experimental 2PPLE peak (black line) and calculated two-photon spectra (red line) from TB. The peaks in (b) and (c) are labeled by the corresponding transitions as calculated using the TB model.

chanical selection rules, determined by the angular momentum L of the exciton wavefunction. For simplicity, assuming that the states of the NC have a definite parity (i.e., spherical symmetry), one-photon processes occur between states with $\Delta L = 0$, while two-photon processes occur between states with $\Delta L = \pm 1$. Thus, 2PPLE spectroscopy accesses an entirely separate manifold of transitions and provides a complimentary set of information to one-photon measurements.

Here, we report investigations of PbSe NC electronic structure using 2PPLE spectroscopy and compare experimental results with the predictions from a TB calculation. For all NC sizes studied, the energy of the two-photon excited transition matches the theoretically predicted $1S_{h,e}-1P_{e,h}$ transition energy. Furthermore, the first two-photon allowed transition occurs close in energy to the second, one-photon absorption peak, suggesting that they should both be assigned as a formally forbidden S–P transition. Dielectric dispersion measurements reveal that PbSe NCs have a negligible internal electric polarization, eliminating a primary source of potential symmetry breaking that could rationalize the strength of the mixed parity transition. Instead, we suggest that quadrupole optical transitions are sufficiently strong to

possibly play a role in explaining the complete one-photon absorption spectrum.

Four PbSe NCs samples from 3–5 nm in diameter were synthesized following literature methods^{6,8} and were characterized by absorption, fluorescence, and one-photon photoluminescence excitation (1PPLE) spectroscopies at 300 K. All samples exhibit photoluminescence quantum yields of $\sim 30\%$ and absorption spectra match those previously reported in the literature.^{7,8} The first absorption peak agrees well with the predicted energy of the $1S_h-1S_e$ transition; the calculated $1P_h-1P_e$ transition is split due to intervalley coupling¹⁰ and the third one-photon absorption peak agrees well with the strongest calculated $1P_h-1P_e$ transition (Figure 1b).

2PPLE measurements at 300 K were performed by wavelength tuning the idler beam of an optical parametric amplifier pumped by a regeneratively amplified Ti:sapphire laser. Excitation wavelengths (between 1600–2500 nm) were determined by reflecting a portion of the signal or idler beam into a spectrometer equipped with an extended InGaAs array detector. Prior to exciting the sample, the laser beam was attenuated by a neutral density filter to achieve average powers of 3–5 mW and then focused onto the sample by a 75 mm lens. Colloidal samples were prepared in a 1 cm cuvette (optical density ~ 0.2) with a small excess of oleic acid as a stabilizer. The excitation wavelength was tuned in 10 meV steps and two-photon emission intensities were normalized by the square of the measured laser power.

Two-photon absorption spectra for two sizes of PbSe NCs (diameter = 3.7 and 4.3 nm) were calculated using second-order perturbation theory.¹⁷ The transition rate per unit time is given by

$$W \propto \sum_{c,v} \left[\sum_i \frac{\langle c | \mathbf{e} \cdot \mathbf{r} | i \rangle \langle i | \mathbf{e} \cdot \mathbf{r} | v \rangle}{E_i - E_v - \hbar\nu} \right]^2 \delta(E_c - E_v - 2\hbar\nu)$$

where $\hbar\nu$ is the photon energy, \mathbf{e} is the polarization vector of the light, c (v) represents the unoccupied (occupied) electronic states of energy E_c (E_v), and the sum inside the bracket is over all the states i , either occupied or empty. The electronic states were previously determined,¹⁰ and the Hamiltonian matrix was written in a $sp^3d^5s^*$ basis while the hopping integrals were restricted to first nearest neighbor interactions. The matrix elements of the dipolar operator $\mathbf{e} \cdot \mathbf{r}$ were derived following ref 10, and the two-photon absorption spectra correspond to averages over the polarization vector \mathbf{e} . Compared to one-photon absorption, the calculation of a two-photon absorption spectrum requires the determination of all the electronic states of the system, increasing the computation time significantly.

The calculated and experimental two-photon spectrum for a NC with a first one-photon peak at 0.911 eV are shown in Figure 1c. The TB calculation models both the energy and line shape of the two-photon $1S_{h,e}-1P_{e,h}$ transition very well. Experimental 2PPLE spectra for all samples measured at the emission maximum are shown in Figure 2a. As expected, the two-photon peak red-shifts with increasing NC size and

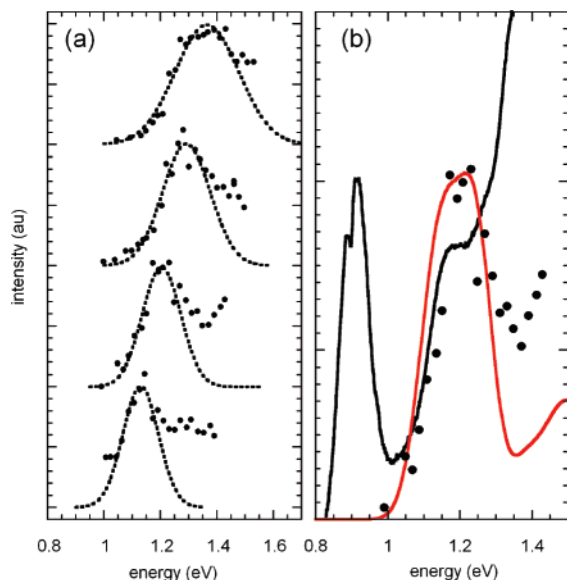


Figure 2. (a) 2PPL spectra of all PbSe NC samples (filled circles) and Gaussian profile fits of the lower energy half of the 2PPL peak. (b) Overlaid one-photon (solid line) and two-photon (filled circles) excitation spectra of one PbSe NC sample, showing the similarity in 1PPL and 2PPL peak energies. The red line is the calculated 2-photon absorption spectrum for a PbSe NC with a first one-photon absorption peak at 0.93 eV. All spectra are measured at the global emission maximum.

in all four samples it is located between the first and third one-photon peaks, at an energy very close to the second one-photon peak (Figure 2b). A small energy difference exists between the $1S_h-1P_e$ and $1P_h-1S_e$ transitions (whose splitting increases with decreasing size), thus suggesting that the two-photon spectrum should have two maxima. However, with the current resolution limits, we were only able to resolve one peak in the 2PPL spectra, whose full width at half-maximum (FWHM) increases with decreasing NC size.

Several experiments were performed to ensure the validity of the 2PPL measurements. First, the emission intensity exhibits the expected square dependence on excitation intensity. As expected, some samples exhibit a saturation of the fluorescence at high-laser intensities ($I \sim 2000 \text{ GW/cm}^2$), so all measurements were performed in the low-intensity regime. Second, fluorescence spectra obtained via two-photon excitation matched those obtained via one-photon excitation. Finally, both 1PPL and 2PPL peaks shift when monitoring only a narrow spectral region of the overall emission spectrum, as expected when tuning across a band edge transition.

Transition energies were obtained by fitting absorption, 1PPL, and 2PPL peaks to a Gaussian profile (after subtracting an increasing polynomial background) and are plotted in Figure 3a. The first 2PPL peak occurs at a slightly greater energy than the second one-photon peak ($39 \pm 12 \text{ meV}$) and shows excellent agreement with the predicted S-P energy level spacing. Following Wehrenberg et al.,⁷ we also calculate the normalized confinement energy versus the first one-photon transition energy for each peak, as shown in Figure 3b. The normalized confinement energy of a transition n is defined as the excess energy above the bulk band gap

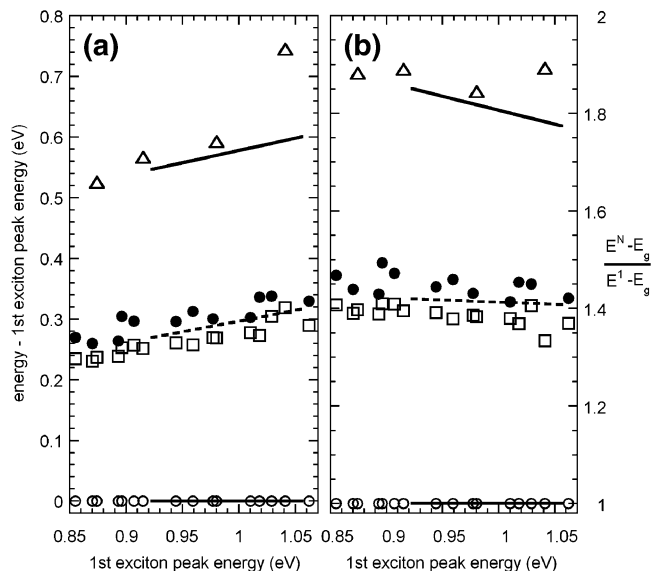


Figure 3. (a) Transition energies and (b) normalized confinement energies for first, second, and third one-photon peaks (open circles, open squares, and open triangles, respectively) and first two-photon peaks (filled circles). Lines are predicted values for one- (solid lines) and two-photon (dashed line) transitions.

E_g , divided by the confinement energy of the first transition: $E_n^{\text{conf}} = (E_n - E_g)/(E_1 - E_g)$. In this manner, each transition is collapsed onto a horizontal line and can be characterized by a single value. The first one-photon peak occurs at a normalized confinement energy of 1.0 (by definition); the average measured values for the second and third one-photon peaks are 1.39 ± 0.02 and 1.88 ± 0.02 , respectively, in agreement with previously published results.⁷ The first two-photon peak, normalized with E_1 of the 1PPL spectrum monitored at the same emission wavelength, occurs at a normalized confinement energy of 1.45 ± 0.02 and is in good agreement with the predicted value of 1.42 for the $1S_{h,e}-1P_{e,h}$ transition.

On the basis of pseudopotential calculations of PbSe NC energy states, the interesting and attractive idea was recently proposed that the anomalous one-photon peak can be explained as an allowed P-P-like transition,¹¹ which is in agreement with STS measurements.¹³ Because the two-photon peak intensity is determined by both the transition strength and the density of allowed transitions in the nearby spectral window, it is possible that the transition we observe in 2PPL is of higher order than the $1S_{h,e}-1P_{e,h}$. However, if the second one-photon transition were a $1P_h-1P_e$ -like transition, one would expect a weaker initial 2PPL transition (i.e., the $1S_{h,e}-1P_{e,h}$) to occur at a smaller energy value than the prominent spectral feature we have measured (corresponding to a normalized confinement energy of ~ 1.2). Despite extensive data analysis, we see no indication of such a weak absorption feature on the low-energy side of the 2PPL peak and therefore must conclude that the observed two-photon peak is in fact the $1S_{h,e}-1P_{e,h}$ transition.

Given this assignment in 2PPL, the similar energies of the second one-photon and first two-photon peaks suggest that they may originate from the same $1S_{h,e}-1P_{e,h}$ transition. Indeed, the energy onset of carrier multiplication,¹ time-

resolved intraband absorption,⁷ the PbSe NC energy gap's size-dependence,⁹ spectroelectrochemical charging,¹⁸ and interband transient absorption measurements¹⁹ are all consistent with the assignment of the second peak as a $1S_{h,c}-1P_{e,h}$ transition. Many of these same measurements have recently been shown to be consistent with alternative models of PbSe NC electronic structure as well;^{11,20} however, the fact that several different experimental observations are consistent with a relatively simple and sparse model of PbSe electronic structure does not seem coincidental. Regardless, a significant challenge remains to determine refinements to the EMA, TB, or pseudopotential models that rationalize the strength of the second peak in the one-photon spectrum in light of these 2PPLE studies.

A natural explanation of the observed large S–P transition strength in CdSe NCs is that the wavefunction symmetry has somehow been broken or altered.²¹ The origin of the symmetry breaking for CdSe NCs is proposed to derive from an internal electric field, caused by the NC's permanent dipole.^{22–24} Although PbSe has no expected dipole due to its cubic lattice symmetry, the existence of a permanent dipole due to (111) faceting has been hypothesized as the driving force for the formation of complex superstructures composed of individual PbSe NCs.²⁵

We tested for the presence of an internal electric field in PbSe NCs by performing dielectric dispersion measurements. CdSe (3.0 nm diameter) and PbSe (5.5 nm diameter) NCs were dispersed in hexadecane, and the complex impedance was measured in the frequency range 10^0 – 10^8 Hz from which the real and imaginary components of the dielectric constant were determined.²⁶ Dielectric dispersion measurements have been previously used to measure dipoles on the order of 30–50 D in CdSe and ZnSe NCs of diameter 3–6 nm.^{23,24} The dipole response of CdSe and PbSe NCs as a function of applied electric field frequency is shown in Figure 4. The relaxation of CdSe NCs at ~ 1 MHz originates from the intrinsic dipole moment of the particles. Following the Debye model,²⁶ the dipolar contribution to the dielectric constant ϵ_d is fit by $\epsilon_d = 4\pi n\mu^2/3kT$ where n is the concentration of NCs, μ is the screened dipole moment, and T is the temperature. The measured CdSe NC relaxation corresponds to a screened dipole of 24 ± 2 D, which is in agreement with previously published results.^{23,24} Completely unexpected, PbSe NCs exhibit no relaxation component. From measured noise levels, we calculate an upper bound for the PbSe NC dipole of <20 D, indicating that the internal electric field in PbSe NCs is at least 3 times smaller than that in CdSe NCs. Therefore, unlike all other semiconductor materials reported to date, symmetry breaking due to an internal electric polarization does not strongly contribute to mixed parity transitions in the PbSe NC one-photon absorption spectrum.

Several additional arguments support the hypothesis that overall symmetry is not broken in the NC. If symmetry breaking permits mixed parity transitions in the one-photon spectrum, conserved parity transitions should be reasonably expected in the two-photon spectrum. In particular, a strong signal at the $1S_e-1S_h$ transition should be visible. However,

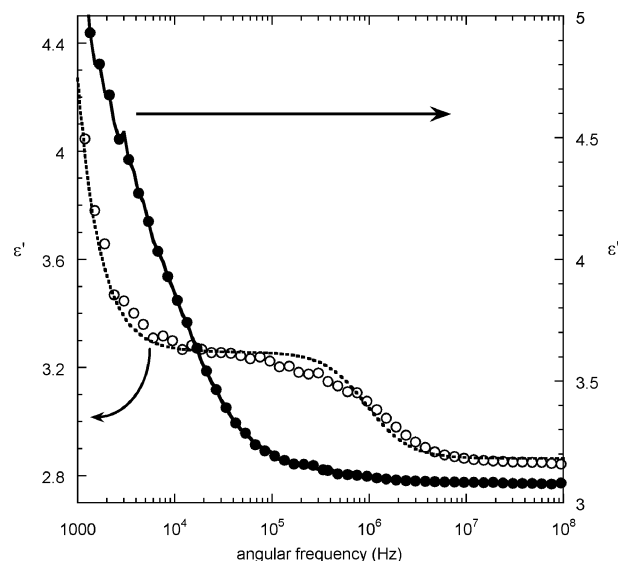


Figure 4. Dispersion measurements of the real component of the dielectric constant (ϵ') for CdSe (open circles, left scale) and PbSe (filled circles, right scale) NCs. The dotted line for CdSe data is the fit to a Debye relaxation at 1.1 MHz corresponding to the dipole response, as described in the text. The CdSe and PbSe scales are slightly offset for clarity.

such transitions were not observed. In addition, calculations of PbSe NCs with a variety of surface reconstructions all fail to reproduce the experimentally observed transition strength of the second peak.¹⁰

Given the negligible internal electric fields, a new physical mechanism must be invoked to explain the presence of mixed parity transitions in the one-photon spectrum. We suggest that the second peak may be the result of unusually strong quadrupole transitions. As described by Zurita-Sánchez and Novotny,²⁷ quadrupole transitions obey the angular momentum selection rule $\Delta L = \pm 1$ and are important in the case of strong electric field gradients, such as those found in near-field optical microscopy. Within the same 4-band EMA formalism, Harbold and Wise have evaluated the interband quadrupole matrix element for an S–P transition in PbSe NCs and concluded that the quadrupole moment is smaller than the dipole moment by a factor of approximately the wavelength of light squared.²⁸ Thus, under far-field excitation, the quadrupole term cannot account for the observed transition strength. However, given the large dielectric constant of PbSe ($\epsilon_\infty = 23$), there exists a significant dielectric discontinuity at the NC surface, causing a large local electric field gradient. Using the local field factor $F = 3\epsilon_1/(\epsilon_2 + 2\epsilon_1)$ where ϵ_1 is the dielectric constant of the surrounding medium (2) and ϵ_2 is the PbSe dielectric (22), one expects the internal electric field to be approximately $\sim 20\%$ of that at the NC surface. Assuming this screening occurs in the first lattice constant of the NC surface, one estimates electric field gradients $|\Delta E/\Delta z| = 0.8 E_0/0.6 \text{ nm} = 1.3 E_0/\text{nm}$, which is comparable to the electric field gradients calculated in a typical near-field excitation scheme $|\Delta E/\Delta z|_{\text{near-field}} = 0.5 E_0/\text{nm}$ ²⁷ and suggests that quadrupole transitions may contribute to the observed transition strength in PbSe NCs. Presently, it is unclear how delocalized

electrons in the NC core would efficiently couple to this surface gradient, but continued theoretical efforts and near-field optical spectroscopy measurements will help to elucidate the role of possible quadrupole transitions.

In summary, two-photon excitation spectroscopy has been used to identify the $1S_{h,c}-1P_{e,h}$ transition energy in PbSe NCs. The observed peak agrees with theoretical predictions from an atomistic TB calculation and supports the picture of a sparse PbSe NC electronic structure. The two-photon transition occurs at energies very close to the second one-photon peak, suggesting that it should be assigned as a formally forbidden S–P transition. Symmetry breaking does not significantly contribute to the forbidden one-photon peak's transition strength, as evidenced by dielectric dispersion measurements and the lack of conserved parity transitions in the two-photon spectrum. Because of the large dielectric discontinuity at the NC surface, quadrupole transitions can be quite strong and may account for the observed transition strength.

Acknowledgment. The authors gratefully acknowledge financial support from the National Science Foundation (CHE 061–6378) and the Camille and Henry Dreyfus Foundation.

References

- (1) Schaller, R. D.; Klimov, V. I. *Phys. Rev. Lett.* **2004**, 92, 186601.
- (2) Ellingson, R. J.; Beard, M. C.; Johnson, J. C.; Yu, P.; Micic, O. I.; Nozik, A. J.; Shabaev, A.; Efros, A. L. *Nano Lett.* **2005**, 5, 865.
- (3) Schaller, R. D.; Petruska, M. A.; Klimov, V. I. *J. Phys. Chem. B* **2003**, 107, 13765.
- (4) Steckel, J. S.; Coe-Sullivan, S.; Bulvic, V.; Bawendi, M. G. *Adv. Mater.* **2003**, 15, 1862.
- (5) Wise, F. W. *Acc. Chem. Res.* **2000**, 33, 773.
- (6) Murray, C. B.; Sun, S.; Gaschler, W.; Doyle, H.; Betley, T. A.; Kagan, C. R. *IBM J. Res. Dev.* **2001**, 45, 47.
- (7) Wehrenberg, B. L.; Wang, C.; Guyot-Sionnest, P. *J. Phys. Chem. B* **2002**, 106, 10634.
- (8) Du, H.; Chen, C.; Krishnan, R.; Krauss, T. D.; Harbold, J. M.; Wise, F. W.; Thomas, M. G.; Silcox, J. *Nano Lett.* **2002**, 2, 1321.
- (9) Kang, I.; Wise, F. W. *J. Opt. Soc. Am. B* **1997**, 14, 1632.
- (10) Allan, G.; Delerue, C. *Phys. Rev. B* **2004**, 70, 245321.
- (11) An, J. M.; Franceschetti, A.; Dudy, S. V.; Zunger, A. *Nano Lett.* **2006**, 6, 2728.
- (12) Kilina, S. V.; Craig, C. F.; Kilin, D.; Prezhdo, O. V. *J. Phys. Chem. C* **2007**, 111, 4871.
- (13) Liljeroth, P.; Zeijlmans van Emmichoven, P. A.; Hickey, S. G.; Weller, H.; Grandidier, B.; Allan, G.; Vanmaekelbergh, D. *Phys. Rev. Lett.* **2005**, 95, 086801.
- (14) Schmidt, M. E.; Blanton, S. A.; Hines, M. A.; Guyot-Sionnest, P. *Phys. Rev. B* **1996**, 53, 12629.
- (15) Blanton, S. A.; Hines, M. A.; Schmidt, M. E.; Guyot-Sionnest, P. *J. Lumin.* **1996**, 70, 253.
- (16) Baranov, A. V.; Masumoto, Y.; Inoue, K.; Fedorov, A. V.; Onushchenko, A. A. *Phys. Rev. B* **1997**, 55, 15675.
- (17) Cohen-Tannoudji, C.; Dupont-Roc, J.; Grynberg, G. *Photons and Atoms: Introduction to Quantum Electrodynamics*; Wiley-Interscience: New York, 1989.
- (18) Wehrenberg, B. L.; Guyot-Sionnest, P. *J. Am. Chem. Soc.* **2003**, 125, 7806.
- (19) Harbold, J. M.; Du, H.; Krauss, T. D.; Cho, K.-S.; Murray, C. B.; Wise, F. W. *Phys. Rev. B* **2005**, 72, 195312.
- (20) Franceschetti, A.; An, J. M.; Zunger, A. *Nano Lett.* **2006**, 6, 2191.
- (21) Schmidt, M. E.; Blanton, S. A.; Hines, M. A.; Guyot-Sionnest, P. *J. Chem. Phys.* **1997**, 106, 5254.
- (22) Colvin, V. L.; Cunningham, K. L.; Alivisatos, A. P. *J. Chem. Phys.* **1994**, 101, 7122.
- (23) Blanton, S. A.; Leheny, R. L.; Hines, M. A.; Guyot-Sionnest, P. *Phys. Rev. Lett.* **1997**, 79, 865.
- (24) Shim, M.; Guyot-Sionnest, P. *J. Chem. Phys.* **1999**, 111, 6955.
- (25) Cho, K.-S.; Talapin, D. V.; Gaschler, W.; Murray, C. B. *J. Am. Chem. Soc.* **2005**, 127.
- (26) Von Hippel, A. R. *Dielectric Materials and Applications*; MIT Press: Cambridge, MA, 1966.
- (27) Zurita-Sánchez, J. R.; Novotny, L. *J. Opt. Soc. Am. B* **2002**, 19, 1355.
- (28) Harbold, J. M. The Electronic and Optical Properties of Colloidal Lead-Selenide Semiconductor Nanocrystals. Ph.D. Thesis, Cornell University, Ithaca, NY, 2004.

NL072487G